Bioorganic Chemistry 83 (2019) 20–28

Contents lists available at ScienceDirect

Bioorganic Chemistry

journal homepage: www.elsevier.com/locate/bioorg

New iridal-type triterpenoid derivatives with cytotoxic activities from *Belamcanda chinensis*

Jiayuan Li, Gang Ni, Li Li, Yanfei Liu, Zhenpeng Mai, Renzhong Wang, Dequan Yu*

State Key Laboratory of Bioactive Substance and Function of Natural Medicines, Institute of Materia Medica, Chinese Academy of Medical Sciences and Peking Union Medical College, Beijing 100050, People's Republic of China

ARTICLE INFO

Keywords:
Belamcanda chinensis
Iridal-type triterpenoids
Cytotoxic activities

ABSTRACT

Eight new iridal-type triterpenoid derivatives, including two noriridals with ether bridge (**1–2**); two iridals lactone (**3–4**), four monocyclic iridals (**5–8**), together with five known iridals (**9–14**) were identified from the rhizome of *Belamcanda chinensis*. Their structures were elucidated on the basis of comprehensive spectroscopic methods and electronic circular dichroism (ECD) calculations. Bioassay results showed that belamcanoxide B (**1**) exhibited moderated cytotoxic activities against HCT-116 and MCF-7 cell lines with IC_{50} values of 5.58 and 3.35 μM.

---

* Corresponding author.
E-mail address: dqyu@imm.ac.cn (D. Yu).

https://doi.org/10.1016/j.bioorg.2018.08.039
Received 25 July 2018; Received in revised form 30 August 2018; Accepted 31 August 2018

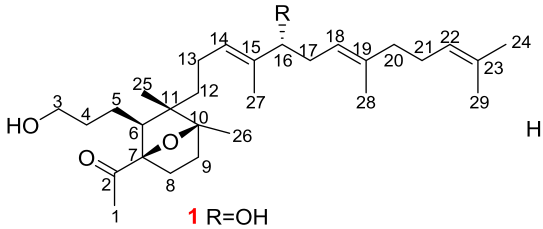

1 R=OH
2 R=CH$_3$COO

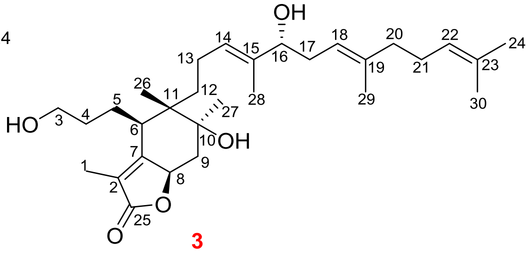

3

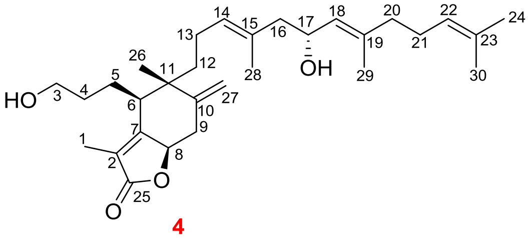

4

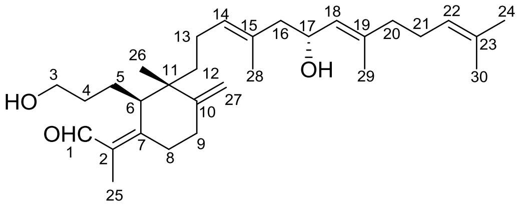

6

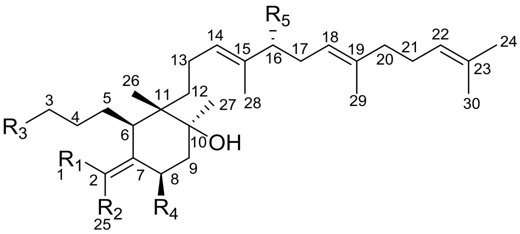

5	R$_1$=CHO	R$_2$=CH$_3$	R$_3$=OH	R$_4$=OH	R$_5$=OH
7	R$_1$=CH$_3$	R$_2$=CH$_3$	R$_3$=OH	R$_4$=H	R$_5$=OH
8	R$_1$=CH$_3$	R$_2$=CHO	R$_3$=CH$_3$COO	R$_4$=H	R$_5$=OH
10	R$_1$=CHO	R$_2$=CH$_3$	R$_3$=OH	R$_4$=H	R$_5$=OH
11	R$_1$=CH$_3$	R$_2$=CHO	R$_3$=OH	R$_4$=H	R$_5$=OH
12	R$_1$=CHO	R$_2$=CH$_3$	R$_3$=OH	R$_4$=H	R$_5$=CH$_3$COO
13	R$_1$=CH$_3$	R$_2$=CHO	R$_3$=OH	R$_4$=H	R$_5$=CH$_3$COO
14	R$_1$=CHO	R$_2$=CH$_3$	R$_3$=CH$_3$COO	R$_4$=H	R$_5$=OH

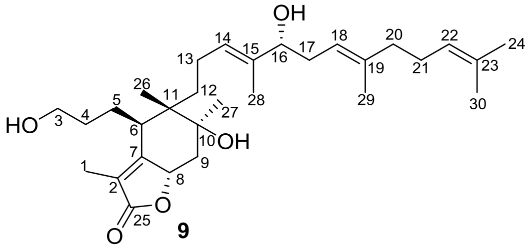

9

1. Introduction

Belamcanda chinensis, a perennial herb belongs to the family of Iridaceae, which is widely distributed in Northeast Asia [1]. Its rhizome has been historically used as a traditional Chinese folk medicine to cure sore throat, bronchitis, and chronic tracheitis due to its effects of heat-clearing, detoxifying and reducing pharyngeal swelling [2]. Pharmacological studies showed that *Belamcanda chinensis* possessed various bioactivities such as anti-inflammatory, anti-oxidative, anti-tumour and oestrogenic activities [3]. To date, abundant secondary metabolites have been isolated from this plant, mainly are isoflavonoids [4] and iridal-type triterpenoids [5,6]. Among them, iridal-type triterpenoids are the characteristic chemical constituents of Iridaceae plants [7], which share a common multisubstituted cyclohexane ring with an α,β-unsaturated aldehyde functional group and a homofarnesyl side chain [8,9]. So far, nearly 100 natural iridals have been reported [7]. Structurally, they all originated from squalene and were divided into five classes: monocyclic iridals, bicyclic iridals [8], spiroiridals [9], polycycloiridals [10] and C$_{16}$-noriridals [11,12]. The fascinating structures and diverse biological activities including anti-inflammation [13], hepatoprotective activity [10,11], neuroprotective activity [14], cytotoxicity [15–17], ichthyotoxicity [18] of iridals have attracted the attention of both organic chemists and pharmacologists [19]. Previously, our research team has been focusing on the structural identification and bioactive evaluation of iridal-type triterpenoids and note that many iridals such as iritectol C [15], belamcanoxide A, iridobelamal A, isoiridogermanal, iridal [16], belamchinenin A [20] and so on, possessed significant cytotoxicities when compared with paclitaxel. This might highlight the value of iridals as templates for the exploration of potential anticancer agents. In our continuing efforts to search for novel cytotoxic and structurally diverse iridals, an investigation was performed on the rhizome of *Belamcanda chinensis* and led to the isolation of eight new compounds. Herein, we reported the isolation, structure elucidation, and cytotoxicity of these components.

2. Materials and methods

2.1. General experimental procedures

Optical rotations were measured by a JASCO P-2000 automatic digital polarimeter. UV spectra were acquired using a JASCO V-650 spectrophotometer. CD spectra were recorded on an Applied Photophysics Chirascan Circular Dichroism Spectrometer. A Nicolet 5700 spectrometer using an FT-IR microscope transmission method was employed to afford IR spectra. NMR was measured with Bruker-400, Bruker-500, and Bruker-600 spectrometers. HRESIMS was afforded using AB SCIEX QTOF MS (QSTAR Elite) and Agilent 6520 Accurate Mass Q-TOF LC/MS spectrometers, respectively. Analytical HPLC was conducted on an Agilent 1260 infinity system equipped with a DAD-UV detector. Preparative HPLC was performed on a CXTH system (Beijing Chuangxintongheng instrument Co. Ltd., P.R. China), equipped with a UV3000 detector using a YMC-Pack ODS-A column (250 × 20 mm, 5 µm, Kyoto, Japan). Column chromatography was performed with Sephadex LH-20 (GE), ODS (50 µm, YMC, Japan), and silica gel (200–300 mesh, Qingdao Marine Chemical Factory, Qingdao, People's Republic of China). TLC was conducted using GF_{254} plates (Qingdao Marine Chemical Factory).

2.2. Plant material

The rhizomes of *Belamcanda chinensis* were collected from Anguo, Hebei Province, P. R. China. A voucher specimen (S-2895) was deposited at Institute of Materia Medica, Chinese Academy of Medical Sciences and Peking Union Medical College.

2.3. Extraction and isolation

The air-dried and powdered rhizomes of *Belamcanda chinensis* (50 kg) were refluxed with 95% ethanol for three times. The extract was evaporated under reduced pressure to give 10 kg residues. The residues were partitioned with dichloromethane (CH_2Cl_2), ethyl acetate (EtOAc) and *n*-butanol (*n*-BuOH) successively. TLC analysis showed that iridal-type triterpenoids mainly distributed in CH_2Cl_2 extract. Subsequently, CH_2Cl_2 extract (1.6 kg) was subjected to a silica gel column and eluted with petroleum/acetone 10:1, 5:1, 3:1, 1:1, 0:1 affording five fractions A-E. Fraction B was dissolved in methanol (MeOH) and filtered to remove the insoluble substance. After that, a MCI column was applied and eluted with MeOH-H_2O (65% to 100%, every five percent as a gradient) to obtain eight fractions B-a to B-h. B-g was chromatographied over a Sephadex LH-20 column with MeOH as eluting solvent to remove part of flavonoids. Following by preparative HPLC afforded 14 subfractions B-g-1 to B-g-14 (MeCN-H_2O 80:20, 10 mL/min). B-g-1 was purified by preparative HPLC with MeOH-H_2O (80:20, 10 mL/min) to obtain compound **1** (10.0 mg, t_R = 42.0 min). Compound **6** (20.3 mg, t_R = 60.2 min) was yielded from subfraction B-g-5 with preparative HPLC (MeOH-H_2O 80:20, 10 mL/min). B-g-3 was subjected to preparative HPLC with solvent system MeOH-H_2O 77: 23 to give compound **8** (10.0 mg, t_R = 59.7 min) and compound **14** (16.4 mg, t_R = 53.9 min). A Sephadex LH-20 column was used to separate fraction B-f into three subfractions B-f-a to B-f-c. B-f-a was isolated by preparative HPLC (MeCN-H_2O 70:30, 10 mL/min) to produce 10 subfractions B-f-a-1 to B-f-a-10. Compounds **10** (8.0 mg, t_R = 37.4 min) and **11** (5.0 mg, t_R = 41.4 min) were isolated by preparative HPLC (MeOH-H_2O 75:25, 10 mL/min) from subfraction B-f-a-6. B-f-a-9 was purified by preparative HPLC (MeOH-H_2O 80:20, 10 mL/min) to obtain compound **7** (1.8 mg, t_R = 81.0 min). B-h was applied to preparative HPLC (MeCN-H_2O 84:16, 10 mL/min) to give 17 subfractions B-h-1 to B-h-17. Subfraction B-h-4 was purified by preparative HPLC (MeOH-H_2O 80:20, 10 mL/min) to afford compound **2** (3.0 mg, t_R = 40.1 min). Compound **3** (2.0 mg, t_R = 65.8 min) was yielded from subfraction B-h-14 with preparative HPLC (MeOH-H_2O 83:17, 10 mL/min). Fraction B-d was applied to a Sephadex LH-20 column and followed by a silica gel column eluting with a gradient of petroleum-isopropanol (40:1, 30:1, 20:1, 10:1, 5:1, v/v) to obtain five fractions B-d-a to B-d-f. B-d-c was further fractioned on an ODS column with a gradient elution (80–100% MeOH in H_2O) to give 10 subfractions B-d-c-1 to B-d-c-10. B-d-c-4 was purified using preparative HPLC (MeOH-H_2O 80:20, 10 mL/min) to afford compound **4** (6.5 mg, t_R = 50.6 min). B-d-c-8 was separated by preparative HPLC (MeOH-H_2O 90:10, 10 mL/min) to yield compounds **13** (9.5 mg, t_R = 43.6 min) and **12** (118.4 mg, t_R = 46.7 min). Fraction C was run on a MCI column with MeOH-H_2O (50% to 100%, every five percent as a gradient), to produce 11 subfractions C-a to C-k. Fraction C-f was applied to a silica gel column and eluted with a gradient of petroleum-isopropanol (40:1, 30:1, 20:1, 10:1, 5:1, = v/v) to obtain five fractions C-f-1 to C-f-5. Fraction C-f-4 was separated by preparative HPLC (MeOH-H_2O 70:30, 10 mL/min) to afford compound **9** (4.0 mg, t_R = 61.3 min). Fraction D was subjected to a silica gel column and used petroleum-isopropanol (20:1, 10:1, 5:1, 3:1, 1:1, = v/v) as eluting solvent to afford five fractions D-a to D-e. Compound **5** (4.0 mg, t_R = 35.8 min) was isolated from fraction D-b by preparative HPLC (MeCN-H_2O 64:36, 10 mL/min).

2.3.1. Belamcanoxide B (1)

Colorless oil; $[\alpha]_D^{20}$ −1.2 (c 0.40, MeOH); UV (MeOH) λ_{max} (log ε) 203 (4.15), 242 (2.94) nm; IR ν_{max} 3414, 2968, 2935, 1709, 1453, 1381, 1059 cm^{-1}; The ^1H NMR and ^{13}C NMR data see Table 1; HRESIMS *m/z* 483.3444 $[M+Na]^+$ (calcd for $C_{29}H_{48}O_4Na$, 483.3445).

2.3.2. 16-O-acetylbelamcanoxide B (2)

Colorless oil; $[\alpha]_D^{20}$ −1.1 (c 0.15, MeOH); UV (MeOH) λ_{max} (log ε) 203 (4.18), 241 (3.41) nm; IR ν_{max} 3423, 2927, 1734, 1709, 1452, 1374, 1055 cm^{-1}; The ^1H NMR and ^{13}C NMR data see Table 1; HRESIMS *m/z* 523.3377 $[M+Na]^+$ (calcd for $C_{31}H_{48}O_5Na$, 523.3394).

2.3.3. Belamcanolide B (3)

Colorless oil; $[\alpha]_D^{20}$ −85.7 (c 0.23, MeOH); UV (MeOH) λ_{max} (log ε) 203 (4.20), 223sh (3.95), 251sh (3.63) nm; IR ν_{max} 3407, 2936, 1731, 1659, 1451, 1379, 1058 cm^{-1}; The ^1H NMR and ^{13}C NMR data see

Table 1
^1H and ^{13}C NMR data for Belamcanoxide B (**1**)[a] and 16-*O*-acetylbelamcanoxide B (**2**)[b].

Position	1		2	
	δ_H, mult (*J* in Hz)	δ_C	δ_H, mult (*J* in Hz)	δ_C
1	2.23, s, 3H	28.4	2.19, s, 3H	28.4
2		211.9		211.9
3	3.49, m	62.9	3.45–3.43, m	62.9
4	1.47–1.42, m	34.0	1.50–1.47, m 1.43–1.39, m	34.0
5	1.47–1.42, m 1.28–1.24, m	25.9	1.43–1.39, m 1.23–1.18, m	25.9
6	1.80–1.75, m	59.7	1.80–1.71, m	59.6
7		94.8		94.8
8	2.21–2.16, m 1.47–1.42, m	33.3	2.15–2.11, m 1.43–1.39, m	33.3
9	1.93–1.89, m 1.81–1.75, m	37.1	1.90–1.85, m 1.80–1.71, m	37.1
10		90.2		90.2
11		50.4		50.4
12	1.47–1.42, m 1.55–1.50, m	41.8	1.43–1.39, m	41.5
13	2.05–2.03, m	25.2	2.06–2.02, m	25.2
14	5.35, t, (7.0)	127.4	5.38, t, (6.7)	129.6
15		138.0		134.2
16	3.94, t, (7.0)	78.6	5.03, m	80.6
17	2.26–2.25, m	34.6	2.36, m 2.26, m	32.4
18	5.09, t, (7.0)	121.7	5.05–4.99, m	120.4
19		137.5		138.9
20	1.99, q, (5.5)	40.9	1.97–1.94, m	40.9
21	2.08, q, (7.6)	27.8	2.06–2.02, m	27.7
22	5.06, t, (7.0)	125.4	5.05–4.99, m	125.2
23		132.2		131.8
24	1.61, s	25.7	1.57, s	25.6
25	1.03, s	17.8	0.98, s	17.8
26	1.33, s	19.0	1.29, s	18.9
27	1.62, s	11.4	1.61, s	12.1
28	1.62, s	16.4	1.60, s	16.4
29	1.68, s	17.8	1.64, s	17.8
1′				172.2
2′			1.98, s	21.2

[a] Recorded at 600 and 150 MHz for ^1H and ^{13}C in CD_3OD.

[b] Recorded at 500 and 125 MHz for ^1H and ^{13}C in CD_3OD.

Table 2
^{1}H and ^{13}C NMR data for Belamcanolide B (**3**)[a] and Belamcanolide C (**4**)[a].

Position	**3**		**4**	
	δ_H, mult (J in Hz)	δ_C	δ_H, mult (J in Hz)	δ_C
1	1.95, s	9.9	1.98, s	9.8
2		121.2		121.6
3	3.65–3.62, m	62.8	3.65, m	62.7
4	1.75–1.70, m 1.59–1.50, m	33.3	1.81–1.74, m 1.52–1.49, m	33.1
5	2.01–1.98, m 1.75–1.70, m	22.9	1.81–1.74, m	21.9
6	2.54, d, (11.5)	47.8	2.50, d, (12.1)	47.0
7		164.8		164.6
8	4.75, ddd, (11.7, 6.2, 1.1)	80.4	4.64, ddd, (10.8, 6.7, 1.1)	82.1
9	2.27–2.22, m 1.59–1.50, m	47.7	3.05, dd, (13.1, 6.7) 2.21–2.18, m	43.3
10		75.2		148.4
11		48.2		46.9
12	1.59–1.50, m	37.5	1.81–1.74, m	37.6
13	2.27–2.22, m 2.18–2.14, m	25.4	2.18–2.08, m 2.03–1.99, m	23.2
14	5.35, t, (7.0)	128.2	5.22, t, (6.8)	128.0
15		137.6		132.8
16	3.94, t, (7.0)	78.8	2.29,dd, (13.2, 6.5) 2.18–2.08, m	49.0
17	2.27–2.22, m	34.7	4.48, dt, (13.9, 8.5, 6.9)	67.8
18	5.10, m	121.8	5.13, m	129.2
19		137.5		138.4
20	2.01–1.98, m	40.9	2.18–2.08, m2.03–1.99, m	40.8
21	2.10–2.06, m	27.8	2.18–2.08, m2.03–1.99, m	27.7
22	5.10, m	125.4	5.13, m	125.2
23		132.1		132.4
24	1.68, s	25.9	1.69, s	25.9
25		177.7		177.6
26	0.87, s	15.4	0.92, s	23.3
27	1.42, s	24.7	5.06, s 4.95, s	112.6
28	1.64, s	11.5	1.67, s	16.8
29	1.63, s	16.4	1.67, s	16.8
30	1.61, s	17.8	1.62, s	17.8

[a] Recorded at 600 and 150 MHz for ^{1}H and ^{13}C in CD_3OD.

Table 2; HRESIMS m/z 511.3390 $[M+Na]^+$ (calcd for $C_{30}H_{48}O_5Na$, 511.3394).

2.3.4. Belamcanolide C (4)

Colorless oil; $[\alpha]_D^{20}$ −55.0 (c 0.20, MeOH); UV (MeOH) λ_{max} (log ε) 203 (3.84), 224sh (3.62), 288sh (2.45) nm; IR ν_{max} 3406, 2928, 1740, 1662, 1632, 1441, 1337 cm^{-1}; The ^{1}H NMR and ^{13}C NMR data see Table 2; HRESIMS m/z 493.3282 $[M+Na]^+$ (calcd for $C_{30}H_{46}O_4Na$, 493.3288).

2.3.5. 8-Hydroxylisoiridogermanal (5)

Colorless oil; $[\alpha]_D^{20}$ -56.0 (c 0.15, MeOH); UV (MeOH) λ_{max} (log ε) 202 (4.06), 246 (3.89) nm; The ^{1}H NMR and ^{13}C NMR data see Table 3; HRESIMS m/z 489.35846 $[M-H]^+$ (calcd for $C_{30}H_{49}O_5$ 489.35855).

2.3.6. Belamcandal A (6)

Colorless oil; $[\alpha]_D^{20}$ +18.9 (c 0.15 MeOH); UV (MeOH) λ_{max} (log ε) 205 (4.26), 257 (3.89) nm; IR ν_{max} 3366, 2972, 1702, 1661, 1445, 1380, 1050 cm^{-1}; The ^{1}H NMR and ^{13}C NMR data see Table 3; HRESIMS m/z 479.3506 $[M+Na]^+$ (calcd for $C_{30}H_{48}O_3Na$, 479.3496).

2.3.7. Belamcandane A (7)

Colorless oil; $[\alpha]_D^{20}$ −7.8 (c 0.15 MeOH); UV (MeOH) λ_{max} (log ε) 204 (4.30), 265 (3.37) nm; IR ν_{max} 3390, 2920, 2852, 1647, 1449, 1376, 1095 cm^{-1}; The ^{1}H NMR and ^{13}C NMR data see Table 3; HRESIMS m/z 483.3821 $[M+Na]^+$ (calcd for $C_{30}H_{52}O_3Na$, 483.3809).

2.3.8. 3-O-acetyliridobelamal A (8)

Colorless oil; $[\alpha]_D^{20}$ + 24.5 (c 0.10, MeOH); UV (MeOH) λ_{max} (log ε) 203 (4.04), 252 (3.85) nm; IR ν_{max} 3420, 2930, 1735, 1657, 1449, 1369, 1043 cm^{-1}; The ^{1}H NMR and ^{13}C NMR data see Table 3; HRESIMS m/z 539.3705 $[M+Na]^+$ (calcd for $C_{32}H_{52}O_5Na$, 539.3707).

2.4. Cytotoxic assay

Cytotoxic activities of all the isolated compounds against HCT-116, HepG2, BGC-823, A549, and MCF-7 cells were measured by using the MTT method. Briefly, test cells in culture medium 100 µL were seeded in each well of 96-well plates (Falcon, CA). Cells were treated in triplicate with 10 µL of grade concentrations 0.1, 1, 10 µM of the compounds at 37 °C. After 72 h, a 20 µL aliquot of MTT solution (5 mg/mL) was added to the wells. The cultures were incubated for another 4 h, and then 100 µL of "triplex solution" (10% SDS/5% isobutanol/10 mM HCl) was added. The plates were incubated at 37 °C in 5% CO_2 overnight. The OD values were measured at 570 nm by a plate reader (VERSA Max, Molecular Devices, Sunnyvale, CA). Average values determined from triplicate readings were used for the inhibitory rate calculation by the formula: $(OD_{control\ well} - OD_{treated\ well})/OD_{control\ well} - OD_{blank\ well} \times 100\%$. The IC_{50} was calculated using Logistic regression from three independent tests. Paclitaxel was used as the positive control with IC_{50} values of 0.03, 0.039, 0.019, 0.043, 0.001 µM, respectively [16,17].

3. Results and discussion

Belamcanoxide B (**1**) was obtained as colorless oil (MeOH). Its molecular formula was determined as $C_{29}H_{48}O_4Na$ by HRESIMS (m/z 483.3444; calcd. 483.3445), which indicated six indices of hydrogen deficiency. The ^{1}H NMR (Table1) spectrum displayed three olefinic protons at δ_H 5.35 (1H, t, J = 7.0 Hz, H-14), 5.09 (1H, t, J = 7.0 Hz, H-18), and 5.06 (1H, t, J = 7.0 Hz, H-22), suggesting the presence of a homofarnesyl side chain; an oxygenated methine group at δ_H 3.94 (1H, t, J = 7.0 Hz, H-16); an oxygenated methylene group at δ_H 3.49 (2H, m, H-3); and seven methyl groups at δ_H 2.23 (CH_3-1), 1.68 (CH_3-29), 1.62 (CH_3-28, 27), 1.61 (CH_3-24), 1.33 (CH_3-26), and 1.03 (CH_3-25). The ^{13}C NMR spectrum showed 29 carbon resonances comprising of one ketone carbonyl at δ_C 211.9 (C-2); six olefinic carbons at δ_C 137.5 (C-19), 138.0 (C-15), 132.2 (C-23), 127.4 (C-14), 125.4 (C-22), and 121.7 (C-18); four oxygenated carbons, including two oxygenated quaternary carbons at δ_C 94.8 (C-7) and 90.2 (C-10), one oxygenated methine at δ_C 78.6 (C-16), and one oxygenated methylene at δ_C 59.7 (C-3). A carbonyl and three double bonds accounted for four degrees of unsaturation, which suggested that compound **1** possessed two-ring system. All of the NMR signals were characteristic of an iridal derivative. However, the signals of the typical α,β-unsaturated aldehyde group were missing. Further analysis of NMR data revealed that it was replaced by an acetyl group, which was verified by HMBC correlations from CH_3-1 to C-2 and 7; from H-6 to C-7, 8, and C-10; from H-8 to C-2, 7, and C-10 (Fig. 1). Moreover, the strong deshielding effects of C-7 (94.8) and C-10 (90.2), downfield shift 15.1 ppm of C-10 compared with the corresponding signal of isoiridogermanal (C-10, δ_C 75.1) (Supporting Information, Fig. S86) [15], might deduce an ether bridge connecting C-7 and C-10. This was in accordance with two remaining degrees of unsaturation. Besides, by comparison with known compound–Irigermanone [21], a noriridal with an ether bridge between C-7 (δ_C 93.6) and C-10 (δ_C 90.1), the similar deshielding effect was observed. Further interpretation of the 2D NMR spectroscopic data enabled the construction of the planar structure of **1**.

The relative configuration of **1** was defined by NOESY correlations (Fig. 2). The NOESY correlations from H-5 to H-1 and H-25, from H-26 to H-25 indicated that H-1/H-5/H-25/H-26 were cofacial arrangement and were assigned as β-orientation. H-6 was α-oriented due to the NOESY correlations from H-12 to H-6 and H-9; from H-6 to H-8. The

Table 3
^{1}H and ^{13}C NMR data for 8-hydroxylisoiridogermanal (**5**)[a], Belamcandal A (**6**)[b], Belamcandane B (**7**)[c], and 3-*O*-acetyliridobelamal A (**8**)[d].

Position	**5**		**6**		**7**		**8**	
	δ_H, mult (*J* in Hz)	δ_C	δ_H, mult (*J* in Hz)	δ_C	δ_H, mult (*J* in Hz)	δ_C	δ_H, mult (*J* in Hz)	δ_C
1	10.23, s, 1H	191.9	10.19, s, 1H	190.5	1.71, m	21.6	1.67, s	11.5
2		134.0		134.2		133.5		131.9
3	3.31, m	61.3	3.56, td, (6.3, 8.0)	62.9	3.49, t, (6.9)	63.8	3.92, t, (8.0)	64.2
3-OH	4.32, t, (5.0)							
4	1.35, m 1.19, m	32.4	1.30–1.21, m	30.9	1.45–1.42, m 1.28–1.25, m	33.6	2.18–2.10, m	26.8
5	2.08, dd, (11.7, 4.3) 1.74, m	27.9	1.43–1.34, m	24.9	2.08–2.02, m 1.94–1.91, m	27.8	1.33–1.28, m	27.4
6	3.43, dd, (11.2, 2.7)	41.2	3.24, dd, (10.8, 4.4)	47.3	2.55, br.d, (11.3)	46.0	2.71, *br*.d, (12.0)	46.8
7		159.0		161.6		124.2		164.4
8	4.79, m	67.8	2.73, m 2.24–2.13, m	28.4	2.36, br.d, (13.8) 2.28–2.24, m	22.1	3.20, br.d, (12.0) 2.45, m	19.6
8-OH	5.56, d, (5.3)							
9	1.86, m	41.1	2.39–2.25, m	32.4	1.67–1.64, m 1.49–1.48, m	38.1	1.60–1.58, m	37.8
10		75.0		148.9		75.2		73.1
10-OH	4.68, s							
11		44.0		44.7		45.0		44.8
12	1.09, td, (6.4, 5.0) 1.03, m	37.1	1.56–1.52, m 1.15–1.14, m	39.3	1.47–1.48, m 1.12–1.10, m	37.9	1.12–1.08, m	36.4
13	1.86, m	21.7	1.93–1.85, m 1.72–1.68, m	22.5	2.00–1.96, m	24.0	1.91–1.84, m	22.5
14	5.08, t, (6.9)	124.7	5.09, m	128.4	5.24, t, (6.9)	128.5	5.09, t, (4.0)	124.9
15		137.0		131.8		137.1		136.9
16	3.70, td, (6.7, 4.4)	75.8	2.10–2.01, m	48.2	3.90, t, (7.0)	78.8	3.73, q, (8.0)	75.9
16-OH	4.53, d, (4.0)							
17	2.03, m	33.8	4.40, m	66.1	2.28–2.24, m	34.5	2.06, t, (4.0)	33.8
18	4.93, t, (7.1)	121.0	5.09, m	127.4	5.04, t, (7.1)	121.6	4.95, t, (4.0)	121.0
19		134.8		138.3		137.8		134.9
20	1.86, m	39.3	2.01–1.93, m	39.6	2.00–1.96, m	40.9	1.91–1.84, m	39.1
21	1.96, m	26.2	2.10–2.01, m	26.5	2.08–2.02, m	27.8	1.97–1.93, m	26.2
22	5.04, t, (7.0)	124.1	5.09, m	124.7	5.10, t, (6.4)	125.4	5.03, t, (8.0)	124.1
23		130.6		131.7		132.1		130.5
24	1.63, s	25.5	1.66, s	25.8	1.68, s	25.9	1.62, s	25.5
25	1.78, s	10.3	1.83, s	11.1	1.71, s	20.4	10.16, s	190.9
26	1.05, s	17.6	1.12, s	21.7	1.03, s	18.5	0.98, s	17.4
27	1.00, s	24.9	4.97, s 4.74, s	111.1	1.07, s	26.3	1.01, s	25.4
28	1.39, s	11.0	1.58, s	16.3	1.59, s	11.3	1.47, s	11.2
29	1.47, s	16.0	1.65, s	16.7	1.60, s	16.4	1.49, s	16.0
30	1.54, s	17.5	1.58, s	17.8	1.68, s	17.8	1.54, s	17.5
1′								170.3
2′							1.96, s	20.7

[a] Recorded at 600 and 150 MHz for ^{1}H and ^{13}C in DMSO-d_6.
[b] Recorded at 400 and 100 MHz for ^{1}H and ^{13}C in $CDCl_3$.
[c] Recorded at 600 and 150 MHz for ^{1}H and ^{13}C in CD_3OD.
[d] Recorded at 400 and 100 MHz for ^{1}H and ^{13}C in DMSO-d_6.

geometries of the double bonds $\Delta^{14(15)}$ and $\Delta^{18(19)}$ were determined to be *E* on the basis of NOESY correlations from H-28 to H-13, from H-14 to H-16, from H-18 to H-20, and from H-29 to H-17. Therefore, the relative configuration of compound **1** was assigned. Based on the biosynthetic considerations, the absolute configuration of typical cyclohexane ring of all the iridals reported so far was ascribed to be (6*R*, 10*S*, 11*S*) [22,23]. Compound **1** may originate from compound **10** which underwent a 1, 4-Michael addition reaction between 10-OH and *α*,*β*-unsaturated aldehyde group forming an ether bridge. Because of the O-substitution at C-7, the absolute configuration of C-6 changed from *R* to *S*. Analysis of the Chem 3D structure and considering the biogenetic pathway of **1**, the attack of 10-OH group to C-7 is only possible from “above” [24]. Thus, C-7 was defined as *R*-configuration. Moreover, C-16 was determined as *R*-configuration for all the hydroxyiridals of monocyclic triterpenoids [25].

In order to further confirm the stereochemistry of **1**, the time-dependent density functional theory (TDDFT) method at B3LYP/6-31 + g (d, p) level in MeOH was performed. As shown in Fig. 3, the calculated ECD curve (6*S*, 7*R*, 10*S*, 11*S*)-**1b** (lacking of the homofarnesyl side chain) matched well with the experimental spectrum, allowing the assignment of the absolute configuration of parent nucleus of **1** to be 6*S*, 7*R*, 10*S*, 11*S*. Thus, comprehensive of the above-mentioned NOESY correlations, biogenetic pathways, and ECD calculations, the structure of compound **1** was determined as depicted.

16-*O*-acetylbelamcanoxide B (**2**) was isolated as colorless oil. Its molecular formula $C_{31}H_{50}O_5$ was determined by HRESIMS (*m/z* 525.35419, $[M+Na]^+$, calc. 525.35505). The NMR data of **2** (Table 1) was very similar to **1**, except for the extra signals of an acetyl moiety (δ_C 172.2, 21.2). The differences mainly reflected on the downfield shifts of H-16 ($\triangle\delta$ 1.1) and C-16 ($\triangle\delta$ 2.0) in ^{1}H and ^{13}C NMR data compared with those of **1**, which suggested that acetyl group was located at C-16. It was further supported by HMBC correlations from H-16 to C-1′, 14, 18, and C-27, and from H-2′ to C-16 and C-1′ (Fig. 2).

Belamcanolide B (**3**) was obtained as colorless oil. It was assigned the same molecular formula as belamcanolide A (**9**) [16] by HRESIMS ($C_{30}H_{48}O_5$, *m/z* $[M+Na]^+$ 511.33896, Calc. 511.3394). ^{1}H NMR spectrum (Table 2) displayed three olefinic protons at δ_H 5.35 (1H, t, *J* = 7.0 Hz, H-14), and 5.10 (2H, m, H-18, 22), seven methyls at δ_H 1.95

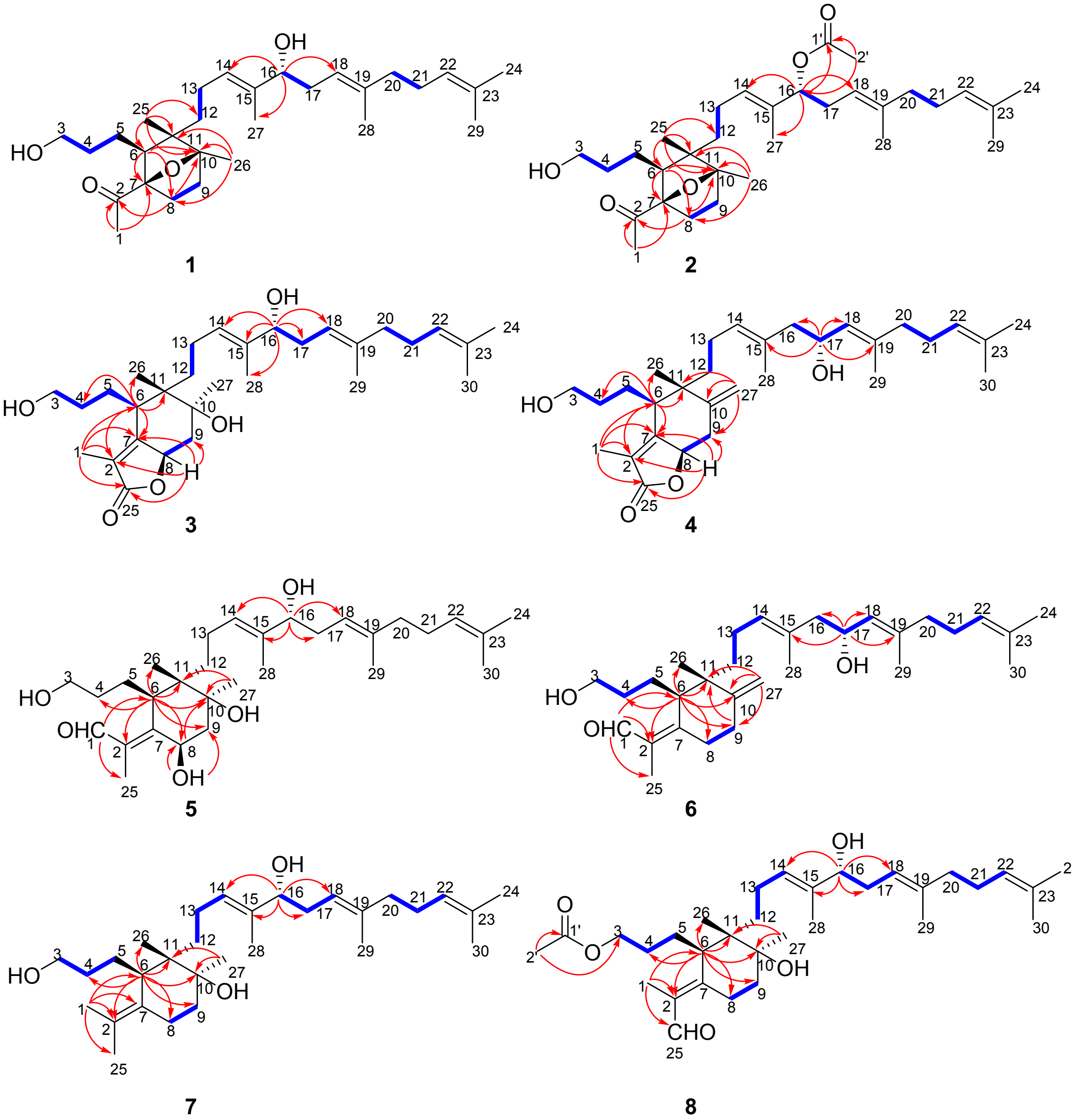

Fig. 1. Selected ^1H–^1H COSY (▬) and HMBC (⌒) correlations of compounds **1–8**.

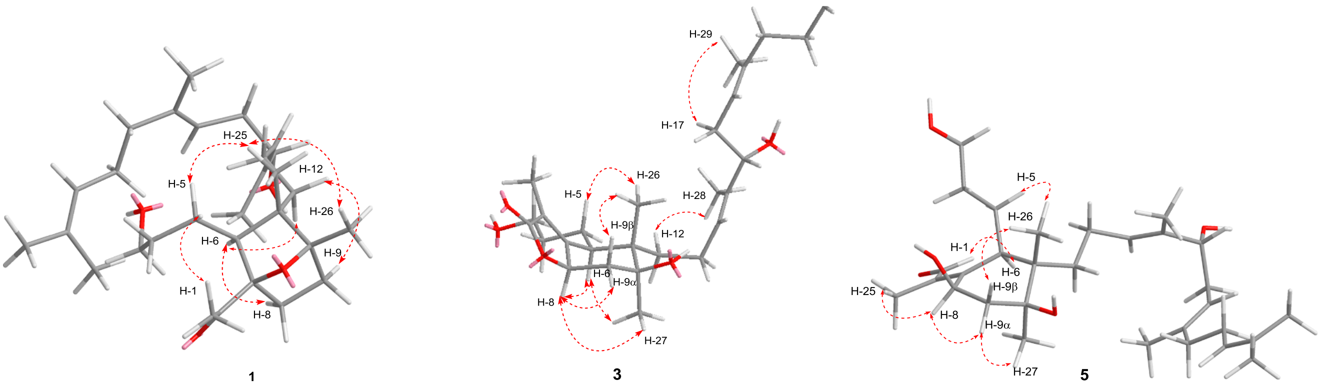

Fig. 2. Key NOESY (⌒) correlations of compounds **1**, **3**, **5**.

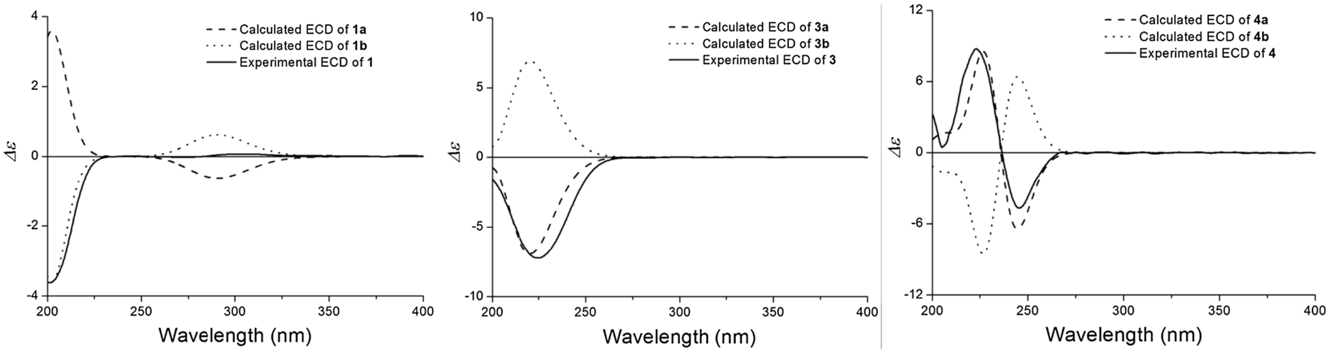

Fig. 3. Comparison of calculated and experimental ECD spectra of compounds **1**, **3**, **4**.

(CH_3-1), 1.68 (CH_3-24), 1.64 (CH_3-28), 1.63 (CH_3-29), 1.61 (CH_3-30), 1.42 (CH_3-27), and 0.87 (CH_3-26), which indicated the presence of a homofarnesyl side chain. Besides, two oxygenated methines at δ_H 4.75 (1H, ddd, J = 11.7, 6.2, 1.1 Hz, H-8), and 3.94 (1H, t, J = 7.0 Hz, H-16), one oxygenated methylene at δ_H 3.65–3.62 (2H, m, H-3) were also observed. ^{13}C NMR spectrum showed 30 resonances including one ester carbonyl, six olefinic carbons, twenty-three aliphatic carbons (four oxygenated carbons). All of the NMR signals implied **3** was an iridal derivative. A combined 1D and 2D NMR analysis showed that **3** and belamcanolide A (**9**) shared the same planar structure. Comparison of the ^1H NMR and ^{13}C NMR data of **3** and **9** (Supporting Information, Fig. 81 and 82), revealed that the differences mainly reflected on chemical shifts of cyclohexane ring and lactone ring (C-2, δ_C 121.2 for **3** *vs* 122.9 for **9**; C-6, δ_C 47.8 for **3** *vs* 45.2 for **9**; C-7, δ_C 164.8 for **3** *vs* 168.5 for **9**; C-8, δ_C 80.4 for **3** *vs* 78.7 for **9**; C-9, δ_C 47.7 for **3** *vs* 44.2 for **9**; C-10, δ_C 75.2 for **3** *vs* 76.9 for **9**; C-11, δ_C 48.2 for **3** *vs* 46.0 for **9**. H-6, δ_H 2.54 for **3** *vs* 2.89 for **9**; H-8, δ_H 4.75 for **3** *vs* 5.18 for **9**). Notably, it was proposed that these differences were attributed to the opposite absolute configuration of C-8. Compounds **3** and **9** were a pair of C-8 epimers. This conclusion was verified by the NOESY correlations (Fig. 2). In NOESY spectrum, the correlations from *α*-oriented H-8 to H-6, H-9*α*, and H-27; from H-6 to H-27 indicated H-6, H-8, H-9*α*, and H-27 were cofacial. While, the NOESY correlations from *β*-oriented H-26 to H-5, and H-9*β* demonstrated H-5, H-9*β*, and H-26 were oriented on the same side. The NOESY correlations from H-28 to H-13, from H-14 to H-16, from H-29 to H-17, and from H-18 to H-20 indicated the geometries of the double bonds $\Delta^{14(15)}$ and $\Delta^{18(19)}$ were *E*. Besides, the split of H-8 [δ_H 4.75 (1H, ddd, J = 11.7, 6.2, 1.1 Hz)] suggested the presence of a long-range coupling (J = 1.1 Hz) between H-6 and H-8 which distributed in a W correlation. This can further confirm the relative configuration of **3**.

The absolute configuration of **3** was further certified by comparison of the experimental ECD spectrum with the calculated ECD spectra of **3a** and **3b** (lacking of the homofarnesyl side chain) by using time-dependent density functional theory calculations at the B3LYP/6-31 + G(d, p) level. Among them, (6*R*, 8*R*, 10*S*, 11*S*)-**3a** and (6*S*, 8*S*, 10*R*, 11*R*)-**3b** were a pair of enantiomers. The experimental ECD spectrum displayed a negative Cotton effect at 224.5 nm, which resulted from the n-π* transition of *α*,*β*-unsaturation lactone moiety. The result showed that the calculated ECD spectrum of (6*R*, 8*R*, 10*S*, 11*S*)-**3a** was compatible with the experimental spectrum (Fig. 3), thus the structure of **3** was established as described.

Belamcanolide C (**4**) was isolated as colorless oil. HRESIMS gave a molecular formula $C_{30}H_{46}O_4$ ($[M+Na]^+$ m/z 493.32822, Calc. 493.32883) with eight indices of hydrogen deficiency. Comparison of the NMR data of **4** with the corresponding signals of **3** (Table 2), it revealed that the structural changes mainly reflected on the terminal double bond and the position of hydroxyl group in side chain. The presence of a terminal double bond signals at δ_H 5.06 (1H, s), 4.95 (1H, s); δ_C 148.4, 112.6 were observed in ^1H and ^{13}C NMR spectra, and the HMBC correlations from H-27 to C-9, 11, and C-10; and from H-9 to C-27 further confirmed the terminal double bond was located at C-10. The ^1H–^1H COSY correlations of H-16/H-17/H-18, along with the HMBC correlations from H-17 to C-15, 16, 18, and 19 supported the presence of 17-hydroxyl (Fig. 2).

The relative configuration of **4** was deduced from the analysis of NOESY correlations. The NOESY correlations from H-8 to H-6, and H-9*α*, from H-6 to H-12, indicated H-6, H-8, and H-12 were *α*-oriented. The *β*-oriented of H-5 and H-26 were established by the NOESY correlations from H-26 to H-5 and H-9*β*. The geometries of two double bonds $\Delta^{14(15)}$ and $\Delta^{18(19)}$ were assigned to be *E* by NOESY correlations from H-28 to H-13, from H-14 to H-16, from H-29 to H-17, and from H-18 to H-20.

The absolute configuration of compound **4** was determined by comparing their experimental and calculated ECD spectra. The experimental ECD spectrum of **4** displayed a positive Cotton effect at 223 nm and a negative Cotton effect at 247 nm (Fig. 3). The calculated ECD curve (6*S*, 8*R*, 11*S*)-**4a** indicated excellent agreement with the experimental spectrum, allowing the assignment of the absolute configuration of **4** as (6*S*, 8*R*, 11*S*). Thus, the structure of **6** was established as shown.

8-Hydroxylisoiridogermanal (**5**) was obtained as colorless oil. Its molecular formula was determined to be $C_{30}H_{49}O_5$ by HRESIMS (m/z 485.35846, $[M-H]^+$; calcd. 489.35855), indicating seven degrees of unsaturation. The ^1H NMR spectrum (Table 3) displayed signals for an aldehyde group at δ_H 10.23 (1H, s, H-1), three olefinic protons at δ_H 5.08 (1H, t, J = 6.9 Hz, H-14), 4.93 (1H, t, J = 7.1 Hz, H-18), and 5.04 (1H, t, J = 7.0 Hz, H-22); two oxygenated methines at δ_H 4.79 (1H, m, H-8), and 3.70 (1H, td, J = 4.4, 6.7 Hz, H-16), one oxygenated methylene at δ_H 3.31 (2H, m), and seven methyls at δ_H 1.78 (CH_3-25), 1.63 (CH_3-24), 1.54 (CH_3-30), 1.47 (CH_3-29), 1.39 (CH_3-28), 1.05 (CH_3-26), and 1.00 (CH_3-27). ^{13}C NMR revealed four oxygenated carbons δ_C 61.3, 67.8, 75.0, and 75.8, which were assigned to C-3, 8, 10 and C-16 through the HSQC correlations, respectively. Comparison of the NMR data with those of isoiridogermanal (**10**) (Supporting Information, Fig. S84), an upfield shift of C-7 (Δ*δ* 6.1) and a downfield shift of C-8 (Δ*δ* 48.1) were observed, which suggested that the hydroxyl group [5.56 (1H, d, J = 5.3 Hz)] was located at C-8. This was further confirmed by HMBC correlations from H-8 to C-10, from 8-OH to C-8 and C-9.

The relative configuration of H-8 was determined by NOESY correlations. The correlations from H-8 to H-25, from H-1 to H-6 indicated that the geometric configuration of $\Delta^{2(7)}$ was *E*. H-8 was assigned to be *α*-orientated via the NOESY correlations from H-8 to H-9*α*, and from H-9*α* to H-27. The NOESY correlations from H-26 to H-5 and H-9*β* were observed, indicating the *β*-orientation of H-5, H-9*β*, and H-26. The absolute configuration of the typical multisubstituted cyclohexane ring of iridals has been determined to be (6*R*, 10*S*, 11*S*) by X-ray analysis and chemical degradation [22,23]. The chiral center formed by hydroxylating at one of the allylic methylene groups of the homofarnesyl side chain has already been determined as (*R*) configuration [25]. Therefore, the absolute configuration of **5** was determined to be (6*R*, 8*R*, 10*S*, 11*S*, 16*R*).

Belamcandal A (**6**) was obtained as colorless oil (MeOH). Its molecular formula was established to be $C_{30}H_{48}O_3$ by HRESIMS data (*m/z* 479.3506, $[M+Na]^+$; calcd. 479.3496), which indicated seven indices of hydrogen deficiency. The UV spectrum displayed an absorption maximum at 256.8 nm. The IR spectrum showed the absorption of carbonyl group at 1702 cm^{-1}. The ^1H NMR spectrum (Table 3) exhibited signals of an aldehyde group at 10.19 (1H, s, H-1), three olefinic protons at 5.09 (3H, m, H-14, 18, 22), a terminal double bond at 4.97 (1H, s, H-27a), and 4.74 (1H, s, H-27b), and six methyls at 1.83 (CH_3-25), 1.66 (CH_3-24), 1.65 (CH_3-29), 1.58 × 2 (CH_3-28, 30), and 1.12 (CH_3-26). Thirty carbon resonances were observed from ^{13}C NMR data, including one aldehyde carbon at δ_C 190.5 (C-1); ten olefinic carbons at δ_C 161.6 (C-7), 148.9 (C-10), 138.3 (C-19), 134.2 (C-2), 131.8 (C-15), 131.7 (C-23), 128.4 (C-14), 127.4 (C-19), 124.1 (C-22), and 111.1 (C-27), including a terminal double band (δ_C 148.9, 111.1); two oxygenated carbons at δ_C 66.1 (C-17), and 62.9 (C-3); and 17 *sp³* carbons. All of the ^1H and ^{13}C NMR data were characteristic of an iridal-type triterpenoid. The NMR data of compound **6** was similar to isoiridogermanal (**10**) [26]. Comparision of the NMR data of compounds **6** and **10**, the most differences were the terminal double bond at C-10 and the position of hydroxyl group in homofarnesyl side chain. The HMBC correlations from H-27 to C-9, 10, and C-11; from H-9 to C-11, and C-27 established the presence of a terminal double bond-$\triangle^{10(27)}$ (Fig. 1). Analysis of the ^1H and ^{13}C NMR data of these two compounds, the different chemical shift of C-16 and C-17 of compounds **6** ($\delta_{H\text{-}17}$ 4.40; $\delta_{C\text{-}16}$ 48.2, $\delta_{C\text{-}17}$ 66.1) and **10** ($\delta_{H\text{-}16}$ 3.92; $\delta_{C\text{-}16}$ 76.7, $\delta_{C\text{-}17}$ 34.2) suggested that the hydroxyl group was located at C-17 of **6**, which was further confirmed by HMBC correlations from H-17 to C-15, 16, 18, and C-19. Biosynthetically, the absolute configuration of the typical multi-substituted cyclohexane ring of iridals has been established as (6*R*, 10*S*, 11*S*) [22,23] and C-16 was assigned to be *R*-configuration [25]. Therefore, compound **6** was identified as shown.

Belamcandane A (**7**) gave a molecular formula $C_{30}H_{52}O_3Na$ on the basis of HRESIMS (*m/z* 483.3821, $[M+Na]^+$; calcd. 483.3809). The ^1H and ^{13}C NMR spectra (Table 3) were found to be close to isoiridogermanal (**10**) (Supporting Information, Fig. S85) [15], except for the aldehyde group at C-2 disappeared and was substituted by a methyl group. In ^1H NMR spectrum, the chemical shifts of H-6 (δ_H 2.55) and H-8 (δ_H 2.36, 2.26) shifted to upfield compared with the corresponding signals of isoiridogermanal ($\delta_{H\text{-}6}$ 3.38; $\delta_{H\text{-}8}$ 2.56, 2.66). This was further confirmed by HMBC correlations from H-1 to C-2, 6, 7 and C-25; and from H-25 to C-1 (Fig. 1). The absolute configurations of C-6, C-10, C-11, and C-16 were determined to be identical with **10**. Thus, the structure of compound **7** was assigned as shown.

3-*O*-acetyliridobelamal A (**8**) was isolated as colorless oil (MeOH). Its molecular formula was established to be $C_{32}H_{52}O_5$ by HRESIMS (*m/z* 539.37054, calcd. 539.37070) indicating seven indices of hydrogen deficiency. Compound **8** exhibited similar NMR data as those of 3-*O*-acetylisoiridogemanal (**14**) (Supporting Information, Fig. 87, 88). In ^1H NMR and ^{13}C NMR spectra (Table 3), an upfield shift of H-8 ($\Delta\delta$ 0.66) and a downfield shift of H-6 ($\Delta\delta$ 0.46), together with an upfield shift of C-8 ($\Delta\delta$ 4.0) and a downfield shift of C-6 ($\Delta\delta$ 4.2) were observed comparing with the corresponding signals of **14**. These differences demonstrated that **8** and **14** were a pair of geometrical isomers of *α,β*-unsaturated aldehyde group. The NOESY correlations from H-8 to the aldehyde group, and from the vinyl methyl to H-6 further confirmed this conclusion.

The known compounds belamcanolide A (**9**) [16], iridobelamal A (**10**) [15,26], isoiridogermanal (**11**) [15,26], 16-*O*-acetyliridobelamal A (**12**) [27], 16-*O*-acetylisoiridogermanal (**13**) [27], and 3-*O*-acetyliridobelamal A (**14**) [27] were elucidated on the basis of ^1H and ^{13}C NMR data comparison with the literature.

Table 4
Experimental data for evaluation of the cytotoxic activities of compounds **1**, **13**, **14**.

Comp.	IC_{50} (μM)				
	HCT-116	HepG2	BGC-823	A549	MCF-7
1	5.58	> 10	> 10	> 10	3.35
13	> 10	7.66	> 10	> 10	6.43
14	8.71	7.22	> 10	> 10	> 10
Paclitaxel	0.003	0.039	0.019	0.043	0.001

In vitro bioactivity assay, the cytotoxic activities of the isolated compounds were measured by MTT method. Compounds **1–14** were evaluated for cytotoxicity against HCT-116, HepG2, BGC-823, A549, and MCF-7 five human cancer cells lines with paclitaxel as a positive control (IC_{50} values of 3, 39, 19, 43, 1 nM, respectively). As shown in Table 4, compound **1** exhibited moderated cytotoxic activities against HCT-116 and MCF-7 cell lines with IC_{50} values of 5.58 and 3.35 μM. Compound **13** displayed moderated cytotoxic activities against HepG2 and MCF-7 cell lines with IC_{50} values of 7.66 and 6.43 μM. Compound **14** showed moderated cytotoxicity against HCT-116 and HepG2 cell lines with IC_{50} values of 8.71 and 7.22 μM. Others were inactive (IC_{50} > 10 μM). This result indicated that the ether bridge moiety, along with the position of aldehyde group and acetyl group may be critical for cytotoxic activities of iridal-type triterpenoids.

4. Notes

The authors declare no competing financial interests.

Acknowledgments

This work was supported by the National Natural Science Foundation of China (No. 21472245), and CAMS Innovation Fund for Medical Sciences (CIFMS, 2016-I2M-1-010).

Appendix A. Supplementary material

Supplementary data to this article can be found online at https://doi.org/10.1016/j.bioorg.2018.08.039.

References

[1] L. Zhang, K.H. Wei, J.P. Xu, D.W. Yang, C.H. Zhang, Z.P. Wang, M.H. Li, J. Ethnopharmacol. 186 (2016) 1–13.

[2] National Pharmacopoeia Committee. Pharmacopoeia of Peoples Republic of China. Part 1. Beijing: Chemical Industry Press, 2015, p. 285.

[3] R.H. Xin, J.F. Zheng, L. Cheng, W.J. Peng, Y.J. Luo, Afr. J. Tradit. Complement. Altern. Med. 12 (2015) 39–70.

[4] O. Monthakantirat, W. De-Eknamkul, K. Umehara, Y. Yoshinaga, T. Miyase, T. Warashina, H. Noguchi, J. Nat. Prod. 68 (2005) 361–364.

[5] H. Ito, S. Onoue, Y. Miyake, T. Yoshida, J. Nat. Prod. 62 (1999) 89–93.

[6] K. Takahashfi, Y. Hoshino, S. Suzuki, Y. Hano, T. Nomura, Phytochemistry 53 (2000) 925–929.

[7] W.W. Gu, G.Y. Xie, Y.S. Xing, M.J. Qin, Drugs & Clinic 31 (2016) 122–130.

[8] F.J. Marner, W. Krick, B. Gellrich, L. Jaenicke, J. Org. Chem. 47 (1982) 13.

[9] F.J. Marner, I. Ritzdorf, G. Johnen, Phytochemistry 33 (1993) 573–579.

[10] C.L. Zhang, Y.F. Liu, Y. Wang, D. Liang, Z.B. Jiang, Z.Y. Hao, H. Luo, G.R. Shi, R.Y. Chen, Z.Y. Cao, D.Q. Yu, Org. Lett. 17 (2015) 5686–5689.

[11] G.R. Shi, X. Wang, Y.F. Liu, C.L. Zhang, G. Ni, R.Y. Chen, D.Q. Yu, Tetrahedron Lett. 57 (57) (2016) 61–5763.

[12] X.L. Chen, X.Q. Zhang, C.A. Geng, T.Z. Li, J.J. Chen, Fitoterapia 124 (2018) 160–166.

[13] C.L. Zhang, Z.Y. Hao, Y.F. Liu, Y. Wang, G.R. Shi, Z.B. Jiang, J. Nat. Prod. 80 (2017) 156–161.

[14] C.L. Zhang, Y. Wang, Y.F. Liu, G. Ni, D. Liang, H. Luo, X.Y. Song, W.Q. Zhang, R.Y. Chen, N.H. Chen, D.Q. Yu, J. Nat. Prod. 77 (2014) 411–415.

[15] C.L. Zhang, Y. Wang, Y.F. Liu, D. Liang, Z.Y. Hao, H. Luo, Q.J. Zhang, G.R. Shi, R.Y. Chen, Z.Y. Cao, D.Q. Yu, Tetrahedron 71 (2015) 5579–5583.

[16] G. Ni, G.R. Shi, J.Y. Li, D.Q. Yu, RSC Adv. 7 (2017) 20160–20166.

[17] G. Ni, J.Y. Li, Z.P. Mai, D.Q. Yu, Tetrahedron Lett. 59 (2018) 151–155.
[18] Y. Miyake, H. Ito, T. Yoshida, Can. J. Chem. 75 (1997) 734–741.
[19] A. Corbu, M. Aquino, T.V. Pratap, P. Retailleau, S. Arseniyadis, Org. Lett. 9 (2008) 1787–1790.
[20] G. Ni, J.Y. Li, Org. Biomol. Chem. 16 (2018) 3754–3759.
[21] O. Potterat, C. Herzog, M. Raith, S.N. Ebrahimi, Helv. Chim. Acta. 97 (2014) 32–38.
[22] F.J. Marner, W. Krick, B. Gellrich, L. Jaenicke, J. Org. Chem. 47 (1982) 2531–2536.
[23] W. Krick, F.J. Marner, B. Gellrich, L. Jaenicke, Helv. Chim. Acta. 67 (1984) 318–324.
[24] A. Littek, F.J. Marner, Helv. Chim. Acta. 74 (1991) 2035–2042.
[25] M. Lamshöft, H. Schmickler, F.J. Marner, Eur. J. Org. Chem. 4 (2003) 727–733.
[26] R. Fang, P.J. Houghton, C. Luo, P.J. Hylands, Phytochemistry 68 (2007) 1242–1247.
[27] F. Abe, R.F. Chen, T. Yamauchi, Phytochemistry 30 (1991) 3379–3382.